Selective Adsorption of Glucose-Derived Carbon Precursor on Amino-Functionalized Porous Silica for Fabrication of Hollow Carbon Spheres with Porous Walls

Shigeru Ikeda,*,† Koji Tachi,† Yun Hau Ng,† Yoshimitsu Ikoma,† Takao Sakata,‡ Hirotaro Mori,‡ Takashi Harada,† and Michio Matsumura†

Research Center for Solar Energy Chemistry, Osaka University, 1-3 Machikaneyama, Toyonaka 560-8531, Japan, and Research Center for Ultra-High Voltage Electron Microscopy, Osaka University, 7-1 Mihogaoka, Ibaraki 567-0047, Japan

Received January 31, 2007. Revised Manuscript Received June 19, 2007

Coating of polysuccharide (PS) generated by hydrothermal treatment of glucose on Stöber's silica particles was examined. Uniform surface coverage of PS was achieved when the silica particles, the surfaces of which had been modified with amino groups, were mixed during the hydrothermal reaction of glucose. On the other hand, bare silica could not be coated with PS upon addition to the hydrothermal reaction solution; instead, this produced spherical PS particles with diameters of a few tens of nanometers beside silica particles. The significant effect of surface amino-functionalization of silica particles on the coverage of PS is attributable to induction of an electrostatic attraction between the positively charged amino-functionalized silica surface and negatively charged PS. When silica (core)−porous silica (shell) spheres were used instead of Stöber's silica, efficient filling of the pores of the silica shell with PS could also be achieved by amino-functionalization of the surface of the porous silica shell. The silica (core)−PS (shell) materials as-obtained were converted into isolated hollow carbon spheres with well-developed porous shell structures by heat treatment under a vacuum followed by treatment with aqueous hydrofluoric acid.

Introduction

Carbon materials with tailored pore systems have received a great deal of attention because of their diverse applications, including adsorbents, materials for gas separation, catalyst supports, electrodes for double-layer capacitors and fuel cells, sensors, and storage materials.[1−6] The development of various methods for fabricating these nanometer-sized carbons has therefore become one of the most technologically important subjects.[2−19] Remarkable progress has been achieved by a replication method using silica-based solid templates,[7] such as silica colloids,[8,9] zeolites,[10] ordered mesoporous silicas,[3−5,11−14] and opals,[6] for the synthesis of porous carbons with various pore sizes and porosities.

Templating approaches for fabrication of porous carbons are based on the carbonization of polymers preformed in the pores followed by removal of the used template material. Various carbon sources such as sucrose, furfuryl alcohol, ethylene gas, mesophase pitches, in situ polymerized phenol resin, and aromatic compounds can be used under suitable

* Corresponding author. Tel.: 81-6-6850-6696/6699. Fax: 81-6-6850-6699. E-mail: sikeda@chem.es.osaka-u.ac.jp.
† Research Center for Solar Energy Chemistry, Osaka University.
‡ Research Center for Ultra-High Voltage Microscopy, Osaka University.

(1) (a) Subramoney, S. *Adv. Mater.* **1998**, *10*, 1157−1171. (b) Kyotani, T. *Carbon* **2000**, *38*, 269−286.
(2) Han, S.; Sohn, K.; Hyeon, T. *Chem. Mater.* **2000**, *12*, 3337−3341.
(3) (a) Vinu, A.; Streb, C.; Murugesan, V.; Hartmann, M. *J. Phys. Chem. B* **2003**, *107*, 8297−8299. (b) Vinu, A.; Miyahara, M.; Sivamurugan, V.; Mori, T.; Ariga, K. *J. Mater. Chem.* **2005**, *15*, 5122−5127.
(4) Yang, H.; Yan, Y.; Liu, Y.; Zhang, F.; Zhang, R.; Meng, Y.; Li, M.; Xie, S.; Tu, B.; Zhao, D. *J. Phys. Chem. B* **2004**, *108*, 17320−17328.
(5) Joo, S. H.; Choi, S. J.; Oh, I.; Kwak, J.; Liu, Z.; Terasaki, O.; Ryoo, R. *Nature* **2001**, *412*, 169−172.
(6) (a) Yu, J.-S.; Kang, S.; Yoon, S. B.; Chai, G. *J. Am. Chem. Soc.* **2002**, *124*, 9382−9383. (b) Chai, G. S.; Yoon, S. B.; Yu, J.-S.; Choi, J.-H.; Sung, Y.-E. *J. Phys. Chem. B* **2004**, *108*, 7074−7079.
(7) Lee, J.; Kim, J.; Hyeon, T. *Adv. Mater.* **2006**, *18*, 2073−2094.
(8) (a) Li, Z.; Jaroniec, M. *J. Am. Chem. Soc.* **2001**, *123*, 9208−9209. (b) Fuertes, A. B.; Centeno, T. A. *J. Mater. Chem.* **2005**, *15*, 1079−1083.
(9) (a) Han, S.; Hyeon, T. *Chem. Commun.* **1999**, 1955−1956. (b) Jang, J.; Lim, B. *Adv. Mater.* **2002**, *14*, 1390−1393. (c) Chen, D.-W.; Chang-Chien, C.-Y.; Lin, H.-P.; Lin, Y.-P.; Tang, C.-Y. *Chem. Lett.* **2004**, *33*, 1574−1575.
(10) (a) Enzel, P.; Bein, T. *Chem. Mater.* **1992**, *4*, 819−824. (b) Johnson, S. A.; Brigham, E. S.; Ollivier, P. J.; Mallouk, T. E. *Chem. Mater.* **1997**, *9*, 2448−2458. (c) Ma, Z.; Kyotani, T.; Tomita, A. *Chem. Commun.* **2000**, 2365−2366.
(11) (a) Ryoo, R.; Joo, S. H.; Jun, S. *J. Phys. Chem. B* **1999**, *103*, 7743−7746. (b) Jun, S.; Joo, S. H.; Ryoo, R.; Kruk, M.; Jaroniec, M.; Liu, Z.; Ohsuna, T.; Terasaki, O. *J. Am. Chem. Soc.* **2000**, *122*, 10712−10713. (c) Ryoo, R.; Joo, S. H.; Kruk, M.; Jaroniec, M. *Adv. Mater.* **2001**, *13*, 677−681. (d) Yu, C.; Fan, J.; Tian, B.; Zhao, D.: Stucky, G. D. *Adv. Mater.* **2002**, *14*, 1742−1745. (e) Yoon, S. B.; Kim, J. Y.; Kooli, F.; Lee, C. W.; Yu, J.-S. *Chem. Commun.* **2003**, 1740−1741. (f) Kruk, M.; Jaroniec, M.; Kim, T.-W.; Ryoo, R. *Chem. Mater.* **2003**, *15*, 2815−2823.
(12) (a) Yoon, S. B.; Kim, J. Y.; Yu, J.-S. *Chem. Commun.* **2001**, 559−560. (b) Yoon, S. B.; Kim, J. Y.; Yu, J.-S. *Chem. Commun.* **2002**, 1536−1537. (c) Kim, T.-W.; Solovyov, L. A. *J. Mater. Chem.* **2006**, *16*, 1445−1455.
(13) (a) Kim, T.-W.; Park, I.-S.; Ryoo, R. *Angew. Chem., Int. Ed.* **2003**, *42*, 4375−4379. (b) Fuertes, A. B.; Alvarez, S. *Carbon* **2004**, *42*, 3049−3055. (c) Kim, C. H.; Lee, D.-K.; Pinnavaia, T. J. *Langmuir* **2004**, *20*, 5157−5159.
(14) (a) Vix-Cuterl, C.; Boulard, S.; Parmentier, J.; Werckmann, J.; Patarin, J. *Chem. Lett.* **2002**, *31*, 1062−1063. (b) Xia, Y.; Mokaya, R. *Adv. Mater.* **2004**, *16*, 1553−1558. (c) Xia, Y.; Mokaya, R. *Chem. Mater.* **2005**, *17*, 1553−1560.
(15) Tamai, H.; Sumi, T.; Yasuda, H. *J. Colloid Interface Sci.* **1996**, *177*, 325−328.

10.1021/cm0702969 CCC: $37.00 © 2007 American Chemical Society
Published on Web 07/31/2007

conditions to render carbon walls with amorphous or graphitic[4,8,13,14] frameworks for desired applications. The pores of templates are generally filled with such carbon precursors by simple liquid impregnation or chemical vapor deposition,[14] without providing additional attraction between the agents and the surface of the silica template. Thus, special attention was not given to the effect of such interactions in most works. However, some studies have shown the effectiveness of specified surface modifications of the silica template, including implantation of Al acid catalysts to induce polymerization,[12c,13a] loading of trimethylsilyl groups to provide hydrophobicity,[12a,12c] and chemical bonding of monomer molecules,[9b] to achieve efficient filling with carbon precursors, resulting in the formation of carbons with desired structures.

Recently, Yoon and co-workers reported fabrication of hollow carbons with a well-developed porous structure in their shells (*hp*Cs) by using a silica sphere with a nonporous core−mesoporous shell structure as a template.[17] The new hollow carbon nanostructure could offer advantages in catalysis when a metal catalyst is loaded in the shell because it allows a greater degree of catalyst dispersion and provides an open network around the active catalyst for a facile diffusion of reactant(s) and product(s). Indeed, it has been proved that the *hp*C material acts as an excellent support for electrode catalysts in a direct methanol fuel cell upon loading with Pt and Ru catalysts.[18] Our group has studied fabrication of *hp*Cs encapsulated with Pt nanoparticles in their hollow spaces.[19] Because the *hp*C not only acts as a barrier to prevent coalescence between Pt nanoparticles but also provides a void space where organic transformation occurs on the naked surface of the Pt nanoparticle, the material works as an efficient catalyst for various hydrogenation reactions.

The fabrication of these *hp*Cs has been performed by following the procedure for fabrication of porous carbons as described above. However, the *hp*C materials thus-obtained are incompletely isolated in some cases, i.e., some or most parts are aggregated, though this structural property has not been emphasized. Hence, an alternative synthesis including further regulations for controlling resulting carbon shell structures is needed for the fabrication of isolated and well-dispersed *hp*Cs.

The methodology for fabricating porous carbons described above leads to a strategy for producing isolated *hp*C spheres by providing an effective attraction between the solid template and the carbon precursor to induce selective deposition of the precursor into pore systems in the template. The first topic chosen in this study is therefore effects of surface amino-functionalization of silica templates on selective deposition of a glucose-derived carbon precursor. We found that efficient deposition of the precursor could be induced by electrostatic attraction between the positively charged surface of amino-functionalized silica and negatively charged carbon precursor in a certain pH region. By applying this finding, we fabricated the desired isolated *hp*Cs using amino-functionalized silica spheres with nonporous core−porous shell structures as templates. Possible control of the shell thicknesses of resulting *hp*Cs is also discussed.

Experimental Section

Preparation of Silica Particles. Spherical silica particles with an average diameter of 200 nm (*n*SiO_2) were prepared by Stöber's method, which involves base-catalyzed hydrolysis of tetraethyl orthosilicate (TEOS) in a water−ethanol mixture.[20] Ethanol (181 cm^3), water (65 cm^3), and 4.5 cm^3 of aqueous ammonia (28%) were added to an Erlenmeyer flask of 500 cm^3 in capacity. After the addition of 70 mmol of TEOS, the mixture was shaken at a rotation rate of 110 rpm using an EYELA NTS-4000 reciprocal shaker for 2 h at 300 K. White products as produced were collected by centrifugation (15 000−20 000 rpm, 15 min) and redispersed in pure ethanol at least twice to remove unreacted TEOS. The final precipitates were dried at 383 K under vacuum.

Preparation of Silica Particles with a Nonporous Core−Porous Shell Structure. Spherical silica particles having a nonporous core−porous shell (*n*SiO_2@*p*SiO_2) were prepared by successive growth of a nonporous silica core and a porous silica shell, as reported in the literature.[17] The silica core was obtained by the same procedure as that used for preparing *n*SiO_2. To a mixed solution of ethanol (37 cm^3) and water (5 cm^3) was added 0.5 g of *n*SiO_2, and the mixture was sonicated for a few minutes. To the stable dispersion of *n*SiO_2 thus-obtained was added aqueous ammonia (28%, 1.1 cm^3), TEOS (15.4 mmol), and octadecyltrimethoxysilane (3 mmol). After the suspension was shaken at a rotation rate of 120 rpm for 2 h at 300 K, solid parts were collected, washed twice with ethanol, and then dried at 383 K under a vacuum. The white powder of *n*SiO_2 covered with alkylsilylated silica thus-obtained was heated in air at 823 K for 6 h to yield *n*SiO_2@*p*SiO_2.

Amino-Functionalization of *n*SiO_2 and *n*SiO_2@*p*SiO_2 Particles. To 24 cm^3 of methanolic solution containing 2.2 mmol of *n*-(2-aminoethyl)-3-aminopropyltrimethoxysilane (AEAP) was added 1.5 g of *n*SiO_2 or *n*SiO_2@*p*SiO_2. After the suspension was stirred for 1 h at room temperature, the amino-functionalized *n*SiO_2 or *n*SiO_2@*p*SiO_2 thus-obtained (designated as NH_2-*n*SiO_2 or NH_2-*n*SiO_2@*p*SiO_2) was collected by centrifugation, washed with ethanol, and dried at 383 K for 3 h under a vacuum.

Hydrothermal Treatment in Aqueous Glucose and Production of Carbon Samples. To 1.25 mol dm^{-3} of aqueous glucose solution was added 0.2 g of NH_2-*n*SiO_2. The suspension was placed in a Teflon-sealed autoclave and maintained at 453 K for 3 h. After isolation of the brown powder by filtration followed by washing with water and ethanol, the hydrothermal treatment was repeated under the same conditions. When NH_2-*n*SiO_2@*p*SiO_2 powder was used, the hydrothermal treatment was conducted only once in various concentrations of aqueous glucose (0.5, 0.75, 1, and 1.25 mol dm^{-3}). The resulting powders were then heated at 1173 K for 1.5 h under a vacuum and subsequently treated with 10% aqueous hydrofluoric acid (HF) to obtain carbon samples. For comparison,

(16) Ng, Y. H.; Ikeda, S.; Harada, T.; Higashida, S.; Sakata, T.; Mori, H.; Matsumura, M. *Adv. Mater.* **2007**, *19*, 597−601.
(17) (a) Yoon, S. B.; Sohn, K.; Kim, J. Y.; Shin, C.-H.; Yu, J.-S.; Hyeon, T. *Adv. Mater.* **2002**, *14*, 19−21. (b) Kim, M.; Yoon, S. B.; Sohn, K.; Kim, J. Y.; Shin, C.-H.; Hyeon, T.; Yu, J.-S. *Microporous Mesoporous Mater.* **2003**, *63*, 1−9.
(18) Chai, G. S.; Yoon, S. B.; Kim J. H.; Yu, J.-S. *Chem. Commun.* **2004**, 2766−2767.
(19) Ikeda, S.; Ishino, S.; Harada, T.; Okamoto, N.; Sakata, T.; Mori, H.; Kuwabata, S.; Torimoto, T.; Matsumura, M. *Angew. Chem., Int. Ed.* **2006**, *45*, 7063−7066.
(20) (a) Stöber, W.; Fink, A.; Bohn, E. *J. Colloid Interface Sci.* **1968**, *26*, 62−69. (b) Takahara, Y. K.; Ikeda, S.; Tachi, K.; Ishino, S.; Ikeue, K.; Sakata, T.; Hasegawa, T.; Mori, H.; Matsumura, M.; Ohtani, B. *J. Am. Chem. Soc.* **2005**, *127*, 6271−6275.

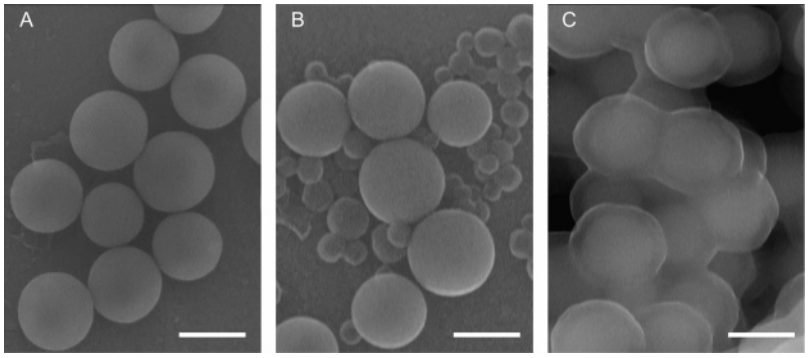

Figure 1. SEM images of nSiO$_2$ (A) before and (B) after hydrothermal treatment with an aqueous glucose solution. (C) SEM image of NH$_2$-nSiO$_2$ after the same hydrothermal treatment. Scale bars correspond to 200 nm.

the above-described hydrothermal treatments were repeated using nSiO$_2$ and nSiO$_2$@pSiO$_2$ instead of NH$_2$-nSiO$_2$ and NH$_2$-nSiO$_2$@pSiO$_2$, respectively.

Characterization and Analytical Procedure. SEM images were taken using a Hitachi S-5000 FEG scanning electron microscope at a voltage of 20 kV. FT-IR spectra were obtained with a Nicolet 470 FT-IR spectrometer equipped with an MCT detector using KBr discs dispersed with the samples. Zeta potentials of nSiO$_2$ and NH$_2$-nSiO$_2$ particles were measured on a Brookhaven Instrument ZetaPALS zeta potential analyzer at 298 K. For these measurements, samples were dispersed in 1 mmol dm^{-3} aqueous NaCl, and the pH of these suspensions was adjusted with NaOH or HCl. TEM images were obtained using a Hitachi H-9000 TEM at a voltage of 300 kV. Thermogravimetry-differential thermal analysis (TG-DTA) was conducted using a Bruker 2000A TG-DTA in air from 300 to 1100 K, using heating ramps of 10 K min^{-1}. Surface and pore analyses were carried out using a Quantachrome AUTOSORB-1 automated gas sorption system employing N_2 as the adsorbate after pretreatment of the sample at 473 K for 2 h. The mean particle size of a carbon sample was determined by using a HORIBA LB-500 dynamic light scattering (DLS) particle analyzer. The measurement was made at 298 K using an aqueous dispersion of the sample containing a dispersant polymer (poly(*N*-vinyl-2-pyrrolidone), M_w = 10,000).

Results and Discussion

Effect of Amino-Functionalization. In a previous study by Sun and Li,[21] glucose was converted into carbonaceous polysaccharide (PS) particles by hydrothermal treatment at temperatures between 433 and 453 K. We have recently found that PS formed a layer to coat particles when certain particles, such as strontium titanate ($SrTiO_3$) and lanthanum oxide (La_2O_3), were present during the hydrothermal treatment.[22] On the basis of these findings, we attempted to coat nSiO$_2$ particles by the same hydrothermal treatment. Panels A and B in Figure 1 show typical SEM images of nSiO$_2$ particles before and after the hydrothermal treatment, respectively. Contrary to our expectation, polymerization of glucose in the presence of nSiO$_2$ did not produce a PS layer on the surface of nSiO$_2$: the morphology of nSiO$_2$ seems to be unchanged from that before the hydrothermal treatment and other spherical PS particles of a few tens of nanometers in size were produced. From the fact that such PS particles were generated without nSiO$_2$ as mentioned above, the surface of nSiO$_2$ did not attract PS, leading to the generation of PS spheres independent of the existence of nSiO$_2$. On the other hand, when hydrothermal treatment of glucose was performed in the presence of NH$_2$-nSiO$_2$, a uniform layer ca. 30 nm in thickness entirely covered NH$_2$-nSiO$_2$ without the formation of such PS particles, as shown in Figure 1C. The FT-IR spectrum of the resulting sample showed absorption bands at ca. 1620, 1710, and 3000−2000 cm^{-1}, corresponding to C═C, C═O, and C−H stretching vibrations, respectively (Figure 2). The other absorption bands in the range between 1300 and 1600 cm^{-1} probably include various modes of vibrations, such as C−O−C symmetric, C−OH stretching, OH bending, those of which overlap one another. Because these absorption bands are identical to those of the PS particle,[21] the surface covered layer on NH$_2$-nSiO$_2$ was composed of PS. Note that additional strong bands below 1300 cm^{-1} are attributable to skeletal vibrations of the Si−O network derived from NH$_2$-nSiO$_2$.

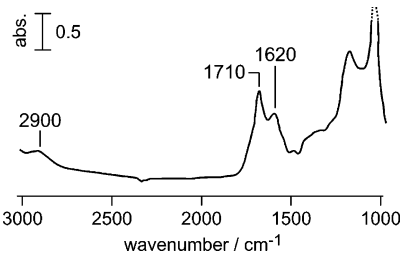

Figure 2. FT-IR spectrum of the NH$_2$-nSiO$_2$ sample after hydrothermal treatment with an aqueous glucose solution.

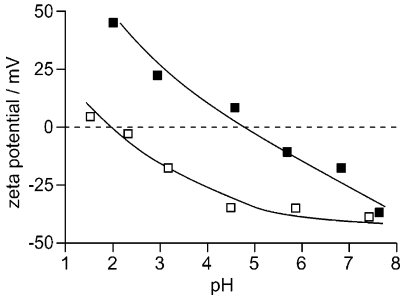

Figure 3. Zeta potential of nSiO$_2$ (open circles) and NH$_2$-nSiO$_2$ (filled circles) as a function of pH.

Figure 3 shows zeta potentials of nSiO$_2$ and NH$_2$-nSiO$_2$ measured at pH values ranging from 1 to 8. The zeta potential of nSiO$_2$ was almost zero at pH 2, consistent with the isoelectric point (IEP) of naked silica particles as reported

(21) (a) Sun, X.; Li, Y. *Angew. Chem., Int. Ed.* **2004**, *43*, 597−601. (b) Sun, X.; Li, Y. *Langmuir* **2005**, *21*, 6019 -6024.
(22) Ikeda, S.; Hirao, K.; Ishino, S.; Matsumura, M.; Ohtani, B. *Catal. Today* **2006**, *117*, 343−349.

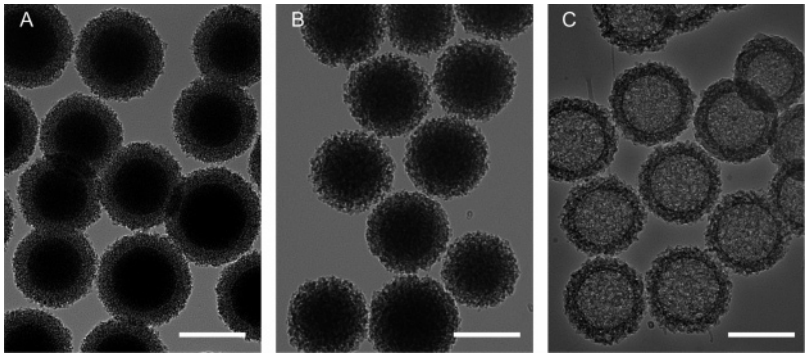

Figure 4. TEM images of NH_2-$n$$SiO_2$@$p$$SiO_2$ (A) before and (B) after hydrothermal treatment with an aqueous glucose solution. (C) TEM image of hollow carbons obtained after heat treatment of PS-deposited NH_2-$n$$SiO_2$@$p$$SiO_2$ particles at 1173 K under evacuation followed by treatment of them with aqueous HF. Scale bars correspond to 200 nm.

previously.[23] Surface amino-functionalization clearly induced a shift of IEP toward a high pH region (ca. 5). Sugimura and co-workers observed a similar upward shift of IEP by a silica substrate modified with an analogous agent of *n*-(6-aminohexyl)-3-aminopropyltrimethoxysilane (AHAP), whereas it gave a higher IEP value (ca. 7.5−8)[24] than that of the present NH_2-$n$$SiO_2$ sample. The relatively small shift of IEP on the present NH_2-$n$$SiO_2$ compared to that in Sugimura's study is likely to be due to incomplete surface coverage of AEAP under the present conditions, resulting in the existence of acidic hydroxyls on the naked surface of $n$$SiO_2$.

During the hydrothermal treatment of aqueous glucose, the pH of the solution changed from approximately neutral to 3−4. As reported in the literature, this is attributable to the presence of appreciable amounts of carboxyl groups on PS.[21,25] The presence of carboxyls is also supported by the existence of the C═O stretching band at 1710 cm^{-1} in the FT-IR spectrum shown in Figure 2. Thus, the observed pH change is a result of the presence of such carboxyls, which should be negatively charged by deprotonation. The surface hydroxyls of $n$$SiO_2$ are also negatively charged at the observed pH region because of the low IEP of $n$$SiO_2$ (ca. 2, see above). In these circumstances, there should be a strong repulsion between $n$$SiO_2$ and PS, resulting in the formation of PS particles beside $n$$SiO_2$. In contrast, because of the relatively high IEP (ca. 5) of the NH_2-$n$$SiO_2$ sample, the surface of NH_2-$n$$SiO_2$ was positively charged by protonation of surface-grafted amino groups at this pH. Moreover, induction of such uniform surface coverage was achieved on the basic metal oxides of $SrTiO_3$ and La_2O_3, the surfaces of which were likely to be positively charged at this pH, though their exact IEPs were not established. Therefore, PS can preferably cover such an amino-functinalized surface through the electrostatic attraction force between NH_2-$n$$SiO_2$ and PS.

Fabrication of Hollow Carbons with Well-Developed Porous Walls. The ability of amino-functionalized surface for selective coverage of the PS layer as mentioned above predicts the efficient filling of PS in the pore system, the surface of which is pretreated with AEAP, leading to the formation of our desired material of *hp*C. On the basis of this idea, we employed $n$$SiO_2$@$p$$SiO_2$, consisting of an $n$$SiO_2$ core 170 nm in diameter and a 46-nm-thick $p$$SiO_2$ shell with mesopores 2.8 nm in diameter (Figure 4A),[17] and the surface of $n$$SiO_2$@$p$$SiO_2$ was amino-functionalized with AEAP.[26] In the same manner as that of PS coating on $n$$SiO_2$ described above, many PS nanoparticles leaving the $n$$SiO_2$@$p$$SiO_2$ particles were produced when original $n$$SiO_2$@$p$$SiO_2$ particles without being functionalized with amino groups were employed, suggesting that there was almost no filling of the pores of $n$$SiO_2$@$p$$SiO_2$ with PS (data not shown). On the other hand, the use of NH_2-$n$$SiO_2$@$p$$SiO_2$ (i.e., amino-functionalized $n$$SiO_2$@$p$$SiO_2$) completely suppressed the formation of such PS particles, as shown in Figure 4B. Although there was almost no change in the morphology after hydrothermal treatment, TG-DTA revealed the presence of large quantities of organic components in the NH_2-$n$$SiO_2$@$p$$SiO_2$ sample after hydrothermal treatment compared with the sample before hydrothermal treatment (see the Supporting Information, Figure S2). These results indicate achievement of efficient filling of PS into the pore system of NH_2-$n$$SiO_2$@$p$$SiO_2$, as we expected.

The NH_2-$n$$SiO_2$@$p$$SiO_2$ sample filled with PS in the porous shell was heated at 1173 K under evacuation and was treated with 10% aqueous HF. Figure 4C shows a typical TEM image of the black powder thus-obtained. In comparison with the sample before this treatment, shown in Figure 4B, the TEM image indicates that the interior of the particle, where NH_2-$n$$SiO_2$@$p$$SiO_2$ originally existed, seems to be vacant without any appreciable changes in the shape and surface morphology of the shell. The fact that the hollow particle vanished upon heat treatment at 873 K in air suggests no residual inorganic component. These results indicate that complete removal of siliceous components should be achieved without losing the PS-derived shell by high-temperature evacuation followed by HF treatment.

A Raman spectrum of the thus-obtained particle exhibited two broad peaks at 1340 and 1600 cm^{-1}. These peaks can

(23) Parks, G. A. *Chem. Rev.* **1965**, *65*, 177−198.
(24) (a) Sugimura, H.; Hozumi, A.; Kameyama, T.; Takai, O. *Surf. Interface Anal.* **2002**, *34*, 550−554.
(25) Luijkx, G. C. A.; van Rantwijk, F.; van Bekkum, H.; Antal, M. J. *Carbohydr. Res.* **1995**, *272*, 191−202.

(26) It is noted that the N_2 sorption isotherm of NH_2-$n$$SiO_2$@$p$$SiO_2$ showed an appreciable decrease in the diameter of pore systems compared to that of the $n$$SiO_2$@$p$$SiO_2$ sample (see the Supporting Information, Figure S1). This indicates achievement of homogeneous modification of the pore wall of the template and the presence of pore systems even after modification. Thus, we used the NH_2-$n$$SiO_2$@$p$$SiO_2$ sample for subsequent studies.

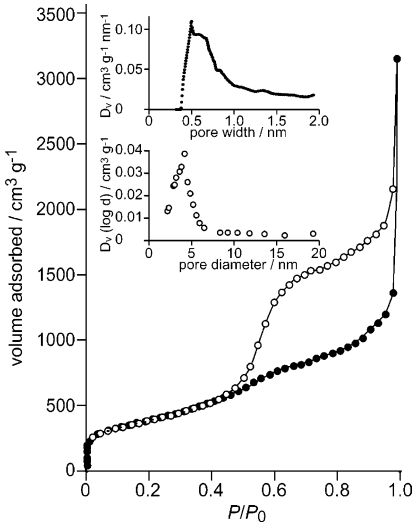

Figure 5. N_2 adsorption−desorption isotherm of the hollow carbon shown in Figure 4C. Filled and open circles denote the adsorption and desorption branches, respectively. Insets denote corresponding micropore size and mesopore size distributions calculated by using the HK (upper) and BJH (lower) formalisms, respectively.

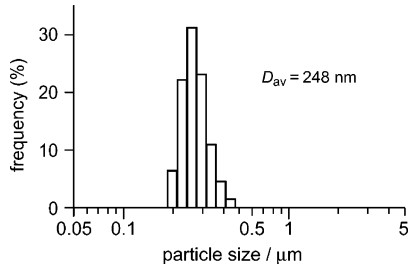

Figure 6. Typical DLS profile of *hp*C measured in aqueous solution containing poly(*N*-vinyl-2-pyrrolidone).

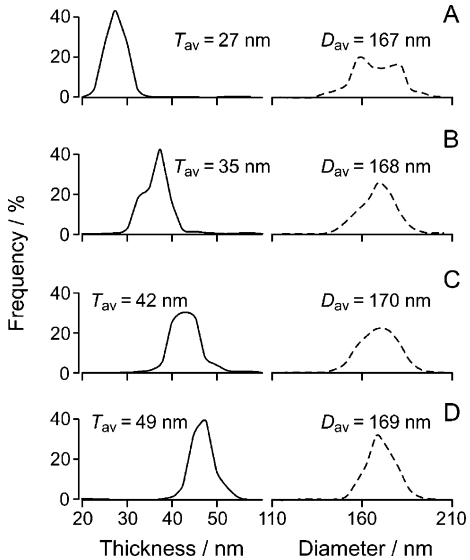

Figure 7. Distributions of thicknesses of carbon shells (solid lines) and diameters of hollow interiors (dotted lines) of *hp*Cs prepared form various concentrations of glucose C_{glu} ((A) 0.5, (B) 0.75, (C) 1, and (D) 1.25 mol dm^{-3}) during the hydrothermal treatment. T_{av} and D_{av} denote average values of thickness and diameter, respectively.

be assigned to in-plane vibration of disordered (amorphous) and crystalline carbon (see the Supporting Information, Figure S3A). Moreover, the powder XRD pattern of the sample exhibits two typical broad reflections (2θ = 10−30°, 35−50°), attributable to C(002) and C(004) reflections

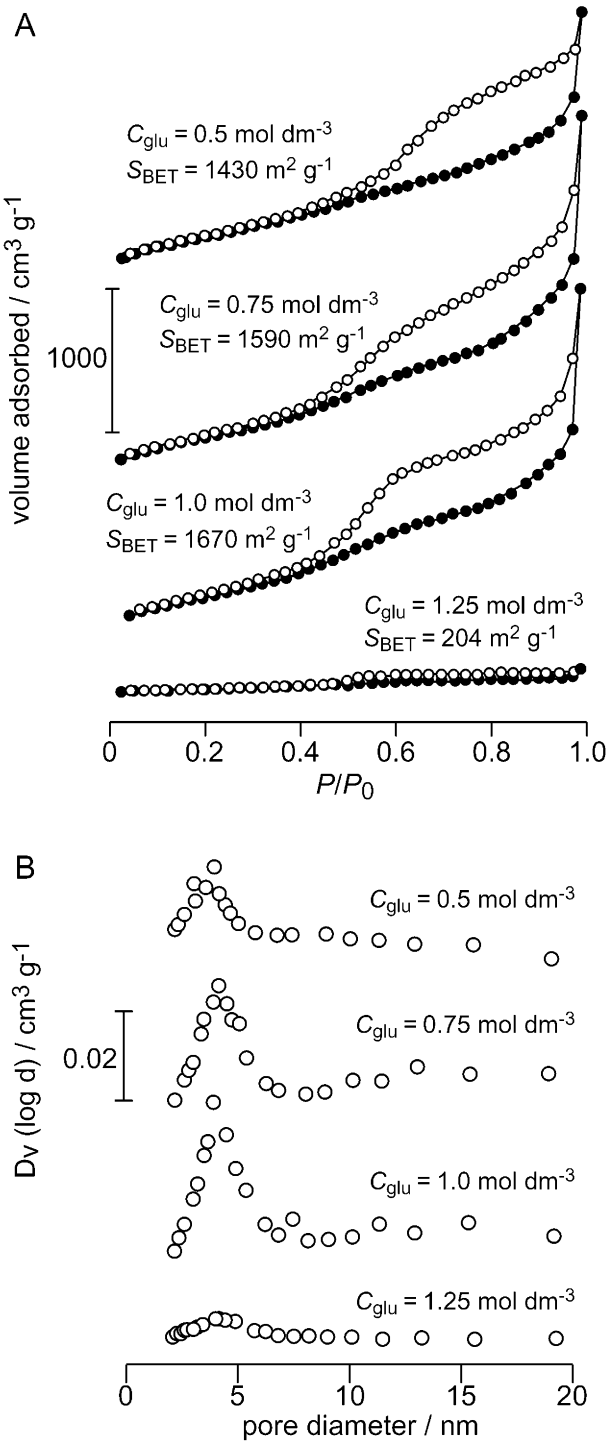

Figure 8. (A) N_2 adsorption−desorption isotherms of *hp*Cs prepared from various C_{glu} during hydrothermal treatment. The meanings of symbols are the same as those in Figure 5. S_{BET} denotes specific surface area obtained by the BET method. (B) BJH pore size distributions of *hp*Cs prepared from various C_{glu} during hydrothermal treatment.

of amorphous carbon composed of polycyclic aromatic carbon sheets oriented in a random manner (see the Supporting Information, Figure S3B).[27] Because such a Raman spectrum and an XRD pattern are generally observed for less-crystalline carbon materials such as activated carbons, the resulting black powder possesses hollow carbons.

(27) (a) Tsubouchi, N.; Xu, C.; Ohtsuka, Y. *Energy Fuels* **2003**, *17*, 1119. (b) Hara, M.; Yoshida, T.; Takagaki, A.; Takata, T.; Kondo, J. N.; Hayashi, S.; Domen, K. *Angew. Chem., Int. Ed.* **2004**, *43*, 2955.

Figure 5 shows an N_2 adsorption−desorption isotherm of the carbonaceous sample. The adsorption branch in the isotherm exhibits a characteristic type IV isotherm, indicating well-developed pore systems. Indeed, the corresponding micropore and mesopore size distributions analyzed from the adsorption branch by applying the Horvath−Kawazoe (HK) and the Barrett−Joyner−Halenda (BJH) formalisms revealed that the sample has micropore and mesopore systems with sizes of 0.4−1.0 and 4 nm, respectively (insets of Figure 5). The specific surface area obtained by application of the Brunauer−Emmett−Teller (BET) method to the isotherm reaches 1670 $m^2\ g^{-1}$, as expected from the results. Another notable feature observed on the isotherm shown in Figure 5 is that the desorption branch in the isotherm denotes a characteristic sudden drop in the volume adsorbed at P/P_0 of ca. 0.5. This phenomenon is often referred to as the tensile strength effect (TSE) and is typically observed in a large pore (mesopore or a macropore) encapsulated by relatively small pore systems.[28] On the basis of these results and considerations, we confirmed successful formation of *hp*C, i.e., a hollow carbon with a well-developed porous structure in the shell, using the present procedure.

It is also notable that the thus-obtained *hp*C forms almost no aggregation between the particles (Figure 4C). In fact, DLS measured in an aqueous suspension containing an appropriate dispersant such as poly(*N*-vinyl-2-pyrrolidone) shows particle size almost comparable to that observed in the above TEM image (Figure 6), indicating the possible achievement of monodispersiblity. Upon dispersion of the *hp*C sample in pure solvents with various polarities, however, such complete dispersion was not obtained. To obtain stable monodispersed suspensions in certain solvents, we probably require either an increase in lyophilicity toward solvents or generation of a repulsive force between the particles by means of loading functional groups on the *hp*C surface. Further studies along this line are now in progress.

Dependence of the Initial Concentration of Glucose on Structures of Resulting *hp*Cs. Figure 7 shows distributions of diameters of hollow interiors and thicknesses of carbon shells of *hp*Cs obtained by the above-described procedure using various concentrations of glucose (C_{glu}) during the hydrothermal treatment. Both size distributions were determined from the corresponding TEM images of samples by measuring more than 100 particles. Despite the fact that there was no increase or decrease in diameter of the hollow interior (ca. 170 nm), the thickness of the carbon shell monotonically increased with an increase in the glucose concentration. Except for the *hp*C sample prepared at high C_{glu} (1.25 mol dm^{-3}), their corresponding N_2 sorption isotherms shown in Figure 8A indicate a gradual increase in the amount of adsorbed N_2 with increase in the thickness of the carbon shell. The specific surface areas calculated by the BET method (S_{BET}) also increased accordingly, but there was no significant change in pore size distributions analyzed by the BJH formalism (Figure 8B). These results imply that the filling of PS is initially completed at the inner part of the pSiO$_2$ shell and advances toward the outer part of the shell, resulting in the formation of a homogeneous porous carbon shell, which inversely replicated the templates at C_{glu} in the hydrothermal process up to 1 mol dm^{-3}. In contrast, the sorption isotherm of the *hp*C sample obtained from relatively high C_{glu} (1.25 mol dm^{-3}) exhibits a significant decline in amount of N_2 adsorbed. From the fact that the thickness of the resulting carbon shell (T_{av} = 49 nm, see Figure 7D) exceeded that of pSiO$_2$ (46 nm) in this condition, the significant drop is attributable to the coverage of a relatively dense carbon layer over the porous carbon shell.

The results described above have proven that selective filling of amino-functionalized surfaces of silica-based templates with a glucose-derived carbon precursor results in the formation of carbon structures that inversely replicated the templates. The isolated *hp*Cs obtained from the concept are applicable to catalyst supports with highly size-selective functionalities for various kinds of reactions when metal nanoparticles, such as platinum, palladium, and rhodium, are fixed inside the carbon shells. The present concept may also be applied to fabrication of trimodal porous hollow carbons, i.e., porous hollow carbons having macroholes on their surfaces, by the use of nSiO$_2$@pSiO$_2$ particles, the surfaces of which are partially modified with amino moieties, as templates. Thus, it is expected that the present method will lead to further development of a new category of porous carbon materials for various applications.

Acknowledgment. This work was supported by a Grant-in-Aid for Scientific Research on Priority Areas (19028042, "Chemistry of Concerto Catalysis") from the Ministry of Education, Culture, Sports, Science and Technology, Japan. Professor Takayuki Hirai (Osaka University) is acknowledged for his stimulating suggestions and discussion. The authors thank Professor Yoshiro Inoue (Osaka University) for his help in zeta potential measurements.

Supporting Information Available: N_2 sorption isotherms of nSiO$_2$@pSiO$_2$ and NH$_2$-nSiO$_2$@pSiO$_2$, TG-DTA curves of NH$_2$-nSiO$_2$@pSiO$_2$ before and after hydrothermal treatment in an aqueous glucose solution, and Raman spectrum and XRD pattern of *hp*Cs (PDF). This material is available free of charge via the Internet at http://pubs.acs.org.

CM0702969

(28) Groen, J. C.; Peffer, L. A. A.; Pérez-Ramírez, J. *Microporous Mesoporous Mater.* **2003**, *60*, 1−17.